Algerian Journal of Environmental Science and Technology
Avril edition. Vol.3. Nº1. (2017)
ISSN : 2437-1114
www.aljest.org

Synthesis and characterization of nano-magnetic material based on (carbon nanotubes / nickel ferrite): Application for the removal of methyl orange dye from contaminated water

K. Seffah [1], N.Bensacia[1*], A. Skender[1, 2], E. Flahaut [3], A. Hadj-ziane-zafour[1]

[1] Laboratoire de Génie Chimique, Université Saad Dahlab de Blida, Algérie
[2] Laboratoire des Materiaux et Environement, Université Yahia Fares Médéa, Algérie
[3] CIRIMAT, Université Paul Sabatier, Toulouse, France

*Corresponding author: polyadsorption@yahoo.fr Tel +213 5 53344549 Fax +213 25 473631

ARTICLE INFO

Article History:

Received ***: 01/01/2017***
Accepted ***: 08/03/2017***

Key Words:

Carbon nanotubes
Adsorption
Methyl orange
Nickel-ferrite

ABSTRACT/RESUME

Abstract: *This work aims the synthesis of (DWNTCs / $NiFe_2O_4$) by refluxing process. Herein, the synthesized adsorbent was characterized via Fourrier Transform Infrared Spectroscopy (FTIR), X-ray diffraction (DRX), BET, zeta potential and transmission electron microscopy (TEM), where the adsorption of methyl orange on (DWNTCs / $NiFe_2O_4$) has been carried out by studying the adsorption kinetics, pH, mass and the initial concentration. The results indicated that the maximum adsorption rate is 7.77 $mg.g^{-1}$ at pH 5 with 100 mg of (DWNTCs / $NiFe_2O_4$), and an initial orange methyl concentration of 10 $mg.l^{-1}$. In addition, the adsorption process describes a second-order kinetic model, where the modeling of adsorption isotherms showed that the Freundlich one seem to be the adequat model describing the adsorption process with $R^2 = 0.97$.*

I. Introduction

Pollution of water by industrial and agricultural activities is a major concern on earth and especially in developed societies. Therefore, high potential of studies has been developed to reduce this pollution at the source or in effluents if it's necessary with appropriate treatments. Among these pollutants, dyes which are used in various fields of industries for various purpose. As a result, large quantities of colored waste water are produced, and the presence of these dyes in water, even at very low concentrations, is highly undesirable and the need for disposal is indispensable [1]. However, various techniques have been developed for decontamination purposes, such as adsorption, degradation, coagulation, precipitation, filtration, electrodialysis, membrane separation and oxidation. However, adsorption process seems to be among the most effective methods yielding therefore to remove dyes from aqueous environments [2], while several studies have already been done in this field using several materials as adsorbents. Indeed, the performance and the efficiency of this adsorption technique depend generally and preponderantly on the nature of the support used as adsorbent.

Thus, nickel-ferrite is a soft ferrite with good magnetic properties and high electrical resistivity [3]. In another side of view, double walled carbon nanotubes shows good mechanical, electrical properties and especially a large surface area [4, 5].

Prior to this, carbon nanotubes are nanomaterials which have undergone considerable development in recent years due to their remarkable potential for nanoscale applications, with a fibrous form, large external surface accessible, and a well-developed mesopore. As a starting point as an hypothesis, the combination of magnetic properties and adsorbent properties within the same material is an interesting challenge that could overcome the problems of recovery of adsorbents loaded with pollutants.

Due to the simplicity of the nanocomposite synthesis composed of double walled carbon nanotubes / nickel-ferrite (DWNTCs/ $NiFe_2O_4$), and

also their preferred properties such as permeability and resistivity, we studied the usefulness of this nanocomposite for the adsorption process. Based on this, this paper briefly addresses this new nanocomposite material for removal of methyl orange from contaminated water.

II. Materials and method

$Fe(NO_3)_3.9H_2O$,$Ni(NO_3)_2.6H_2O$,Sodium ydroxide NaOH was purchased from Panreac Quimica. Concentrated hydrochloric acid (HCl 37%), nitric acid (HNO_3, 65%), sulfuric acid (H_2SO_4, 95%) and methyl orange were supplied by Sigma Aldrich.

II.1.Carbone nanotubes

Double walled carbon nanotubes (DWNTCs) used in this study were synthesized in CIRIMAT (InteruniversityResearch and Materials Engineering Center, Toulouse France) by Catalytical Chemical Vapour Depostion CCVD [6].

II.2.Protocol of synthesis

II.2.1.Purification of DWNTCs

The purification of the double-walled carbon nanotubes is the step of their extraction from the catalyst. The magnesium oxide (MgO)is easily removed by dissolution in concentrated hydrochloric acid (37% HCl). The DWNTCs were purified by HCl and then washed with distilled water several times. Finally, the latter were recovered in a suspension of distilled water.

II.2.2.Oxidation of DWNTCs with HNO_3 / H_2SO_4 mixture

The oxidized DWNTCs were prepared according to the procedure described in the literature [7]. DWNTCs were oxidized with solution of 65% HNO_3 / 95% H_2SO_4 concentrate (1: 3). The suspension was then refluxed at 70 °C for 5 h. After filtration and washing with distilled water, finally the DWNTCs were freeze-dried for 24 hours.

II.2.3. Synthesis of the nanocomposit (DWNTCs/ $NiFe_2O_4$)

5 g and 2.07 g of Fe $(NO_3)_3$,$9H_2O$; $Ni(NO_3)_2$,6H2O respectively were solubilized in 100 mL of distilled water. After this, 10 mL of (9N) NaOH is added in order to have a pH value near 12. 50 mg of DWNTCs oxidized according to the protocol described in prior works [7] was added with stirring, and therefore the solution thus obtained is hydrolysed by heating reflux for 45 min till a black precipitate was formed, which was recovered by centrifugation and rinsed with distilled water several times and then with ethanol. Finally, the resulting product was dried in an oven at 60°C, which will be then ground further.

III. Characterization

The FTIR spectra of the DWNTCs/NiFe2O4 were recorded in the region of 400–4000 cm^{-1} with JASCO 4200. Elsewhere, the powder has been characterized at several stages using X-ray diffraction (XRD), where the XRD patterns were obtained with PANalytical XPERT-PRO diffractometer with Cu Kα radiation (α=1.54059 Å). The specific surface area has been carried out with an automatic Micromeritics Flow Sorb II 2300 using adsorption of nitrogen at his liquid state temperature. As is known, the effect of pH on the variation of the zeta potential (ξ) makes it possible to determine the isoelectric point (PIE). Thereby, zeta potential measurements were achieved with Horiba Scientific Nano Particle Analyzer SZ-100, as a function of the pH, while TGA/dTGA curves were recorded on a TGA Q500 thermogravimetric analyser, which makes it possible to work in a temperature ranging from 25 to 1250 ° C, while the sample was heated from 25 °C to 1000 °C by fixing a thermal rate of 10 °C/ min during the analysis. The transmission electron microscopy (TEM) images were taken with JEOL TEM 1400 device.

IV. Orange methyl adsorption tests on DWNTCs / $NiFe_2O_4$

The adsorption tests were achieved in batch using mass of adsorbent of 100 mg in 100 ml of orange methyl solution as initial concentration (C_0 = 10 $mg.g^{-1}$). After magnetic stirring, solutions were analyzed directly by UV-Vis spectrophotometer (1800 UV SHIMADZU spectrophotometer), at 464 nm.

All solutions are stored away from light and the pH of each ones is adjusted with sodium hydroxide solution (NaOH) at 0.2 N or hydrogen chloride at 0.1 N. The measurements has been done using JENCO pH meter initially calibrated using two buffer solutions (pH = 4 and pH = 7), where the pH of the different solutions varies between 2 and 12. And all adsorption measurements were carried out at 25°C under magnetic stirring at 800 rpm.

The adsorption capacity of the nanocomposite is calculated as follows:

$$Q = \left(\left[(C_0 - C_e\right] \times V\right)/m \quad \ldots\ldots\ldots\ldots\ldots\ldots 1$$

where;

Q is the adsorption capacity ($mg.g^{-1}$), C_0 and C_e are the initial and equilibrium concentrations ($mg.l^{-1}$) respectively, V is the volume of the solution (l) and m is the mass of the adsorbent (g).

IV. Results and Discussions

In first view, preliminary test showed that a mass of the nanomaterial was attracted by the magnet, which confirms therefore the magnetic properties of the synthesized compound.

Elsewhere, the FTIR spectrum of DWNTCs/ $NiFe_2O_4$ (Figure.1) indicates the presence of various functional groups such as C=C (bond between 1430 and 1544 cm^{-1}), C–H of carbons sp^3 (bond between 2846 and 2955 cm^{-1}), =C–H and O–H (towards 3440 cm^{-1}) [7], while the peaks recorded at 450 cm^{-1} and 650 cm^{-1} indicates the tetrahedral and octahedral Fe-O bonds respectively according to previous works [8-11].

X-ray diffraction analysis of the dried and crushed DWNTCs/NiFe2O4 nanomaterial is shown in Figure 2; the diffractogram obtained has been indexed. However, peaks located at 2θ equal to 18.4; 30.3; 35.6; 43.3; 53.5; 57.3 and 62.41 were assigned respectively to the reticular planes (111), (220), (311), (400), (422), (511) and (440), the recording of these peaks indicates the spinel structure of $NiFe_2O_4$ (JCPDS 54-0964) [11-12]. The peak located at 2θ equal to 26 is the typical peak of the carbon nanotubes, and attributed to the reticular plane (002) [14]. From the diffractogram shown in figure 2 and using the relation of Debye Scherrer [15, 16], the mean particle size of the DWNTCs / $NiFe_2O_4$ was found to be of the order of 13 nm.

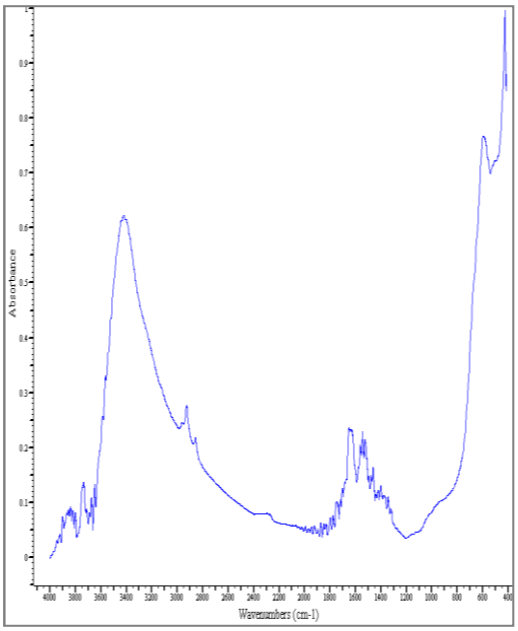

Figure 1. *FTIR spectrum of DWNTCs / $NiFe_2O_4$.*

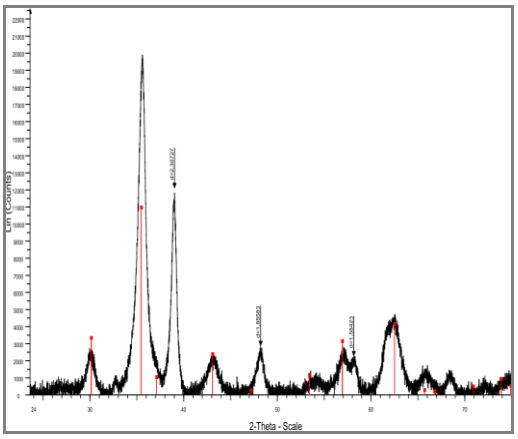

Figure 2. *Diffractograms of the nanomaterial (DWNTCs / Ni-Fe_2O_4).*

Moreover, the Brunauer-Emmett-Teller method (B.E.T) allowed us to determine the specific surface area of the nanomaterial, which has been found to be in the order of 161$m^2.g^{-1}$. As it is well known, the point of zero loads pH (PZC) is a physical parameter corresponding to the pH for which the surface of the solid has a zero charge, in our case, the PZC was found at pH 6. The ATD / ATG thermogram of (DWNTCs / $NiFe_2O_4$) shown in Figure 3, indicates that the estimated mass of the DWNTCs within the nanomaterial is between 5 to10% (w/w). The TEM images shown in Figure 4 indicates that the DWNTCs / $NiFe_2O_4$ is an iron nanocomposite, which represents an entangled network of oxidized carbon nanotubes with clusters of iron oxide nanoparticles attached to the surface.

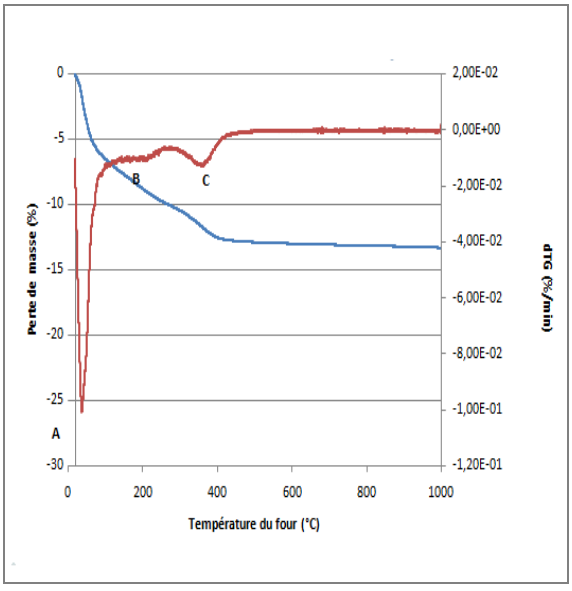

Figure 3. *Thermogram of (DWNTCs / $NiFe_2O_4$)*

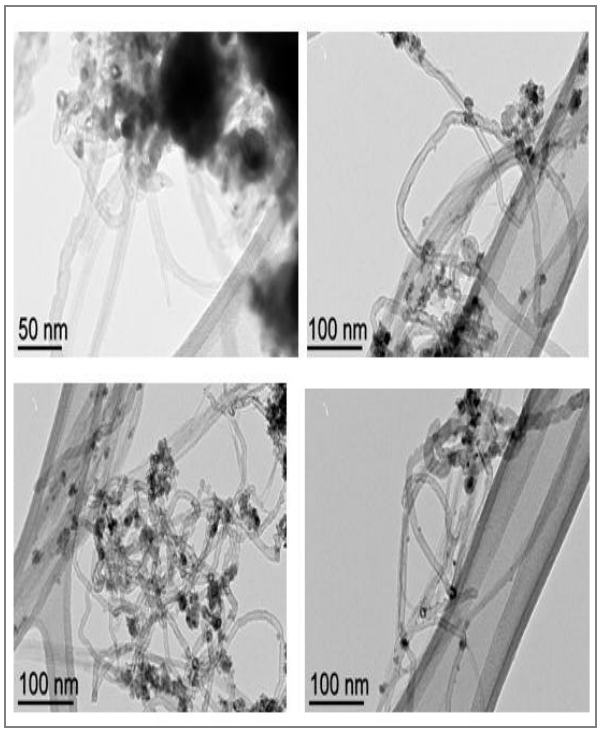

Figure 4. *MET images of (DWNTCs / $NiFe_2O_4$)*

IV.2. Adsorption

IV.2.1. Adsorption kinetics

The adsorption phenomenon depends on several parameters which govern its kinetics such as: agitation of the aqueous phase, structure properties of the adsorbent, the quantity of adsorbent, the initial concentration of the pollutant to be assayed. However, extraction kinetics of methyl orange by the nanocomposite was revealed by taking samples according to specific time intervals of supernatant. The Figure 5 shows the variation of the adsorption capacity as a function of time. As it is presented in Figure 5, the equilibrium time is in the range of 5 h which corresponding therfore to an adsorption capacity of 7.77 mg g^{-1}.

IV.2.2. Effect of pH

The Figure 6 illustrates the variation of the adsorption capacity of (DWNTCs /$NiFe_2O_4$) as a function of pH. As it is shown, we remark clearly that the adsorption capacity increases at pH 5 and then decreases, This can be explained by the fact that when the pH is lower than the isoelectric point of the adsorbent (equal to 6), the surface of the adsorbent is positively charged and the orange methyl is in the form of anions (pka = 3.4), therefore this increase is probably due to the attractive interaction forces between the adsorbent and the adsorbate. Otherwise, the decrease in the adsorption capacity starting at pH 5 is attributed to the repulsive interaction forces between the negatively charged adsorbent and the methyl orange anions.

IV.2.3. Effect of mass

The adsorption experiments were conducted using adsorbent with masses ranging from 5 to 140 mg in solutions with an initial concentration of 10 $mg.l^{-1}$, with a volume of 100 mL. The Figure 7 illustrates the variation of adsorption capacity (Q) as a function of DWNTCs /$NiFe_2O_4$ mass's. As it is shown on Figure 7, it was revealed that when the mass increases the adsorption capacity increases till to equilibrium, where the mass at this stage is equal to 100 mg.

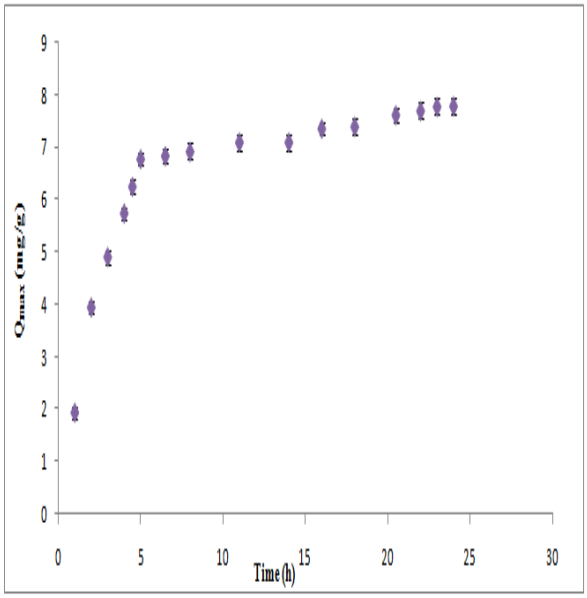

Figure 5. *Orange methyl adsorption capacity on (DWNTCs / $NiFe_2O_4$), pH = 5, m = 100 mg, C_0 = 10 $mg.l^{-1}$*

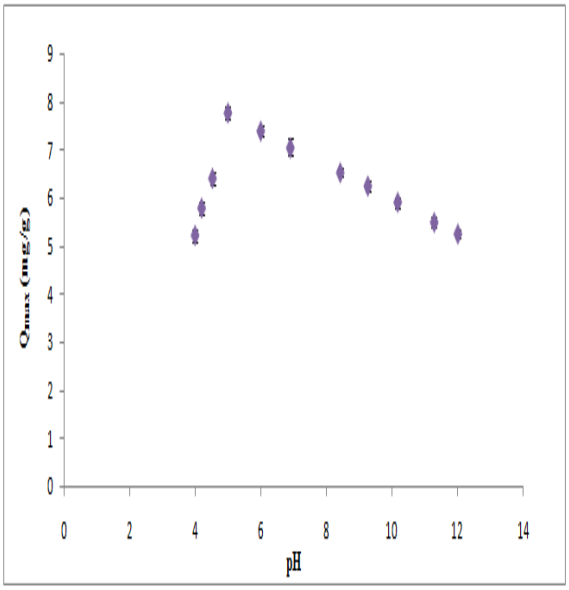

Figure 6. *Effect of pH on the adsorption capacity of orange methyl on (DWNTCs / $NiFe_2O_4$). M = 100mg, C_0 = 10 $mg.l^{-1}$, t = 5h.*

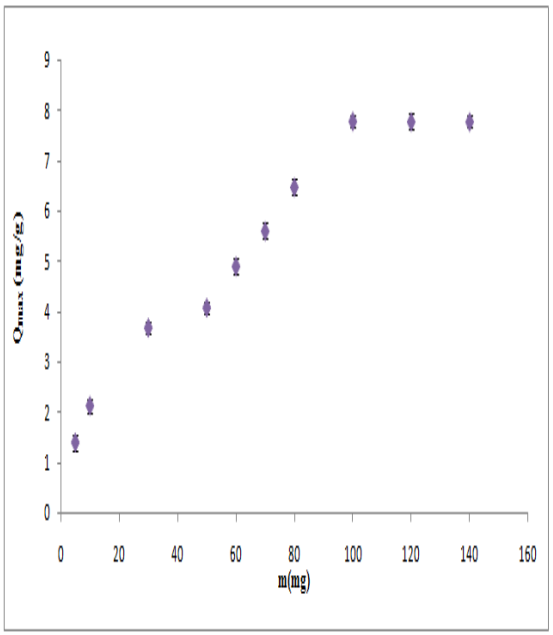

Figure 7. *Effect of the mass of (DWNTCs / $NiFe_2O_4$) on the adsorption of methyl orange. pH = 5, t = 5h, C_0 = 10 mg.l^{-1}.*

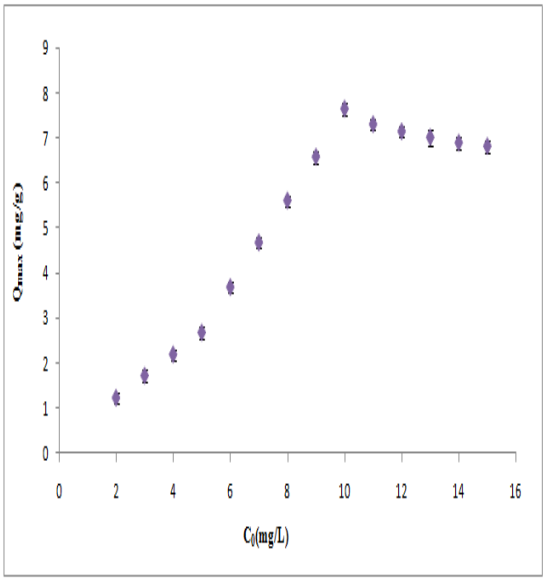

Figure 8. *Effect of the initial concentration of methyl orange on the adsorption capacity of DWNTCs / $NiFe_2O_4$) pH = 5, m = 100 mg, t = 5h.*

IV.2.4. Effect of concentration

The variation of the adsorption capacity as a function of the evolution of the initial concentration is shown in Figure 8. It can be noted, that the adsorption capacity increases with increasing the concentration of methyl orange till to 10 mg.l^{-1}, and therefore the rate becomes constant, where this concentration seem to be an optimal value.

IV.2.5.Comparative study of the adsorption capacity of orange methyl on ($NiFe_2O_4$) and (DWNTCs / $NiFe_2O_4$)

The adsorption tests of orange methyl on nickel ferrite ($NiFe_2O_4$) has been established at 25°C, pH 5 with m = 100 mg and C_0= 10 mg.l^{-1}. It was found that the adsorption capacity of orange methyl on (DWNTCs / $NiFe_2O_4$) is of 7.77 mg.g^{-1} at 25 °C. As a relative comparaison, the (DWNTCs/ NiFe2O4) adsorbs twice better than $NiFe_2O_4$, indicating therfore the high-performance adsorption properties of (DWNTCs / $NiFe_2O_4$).

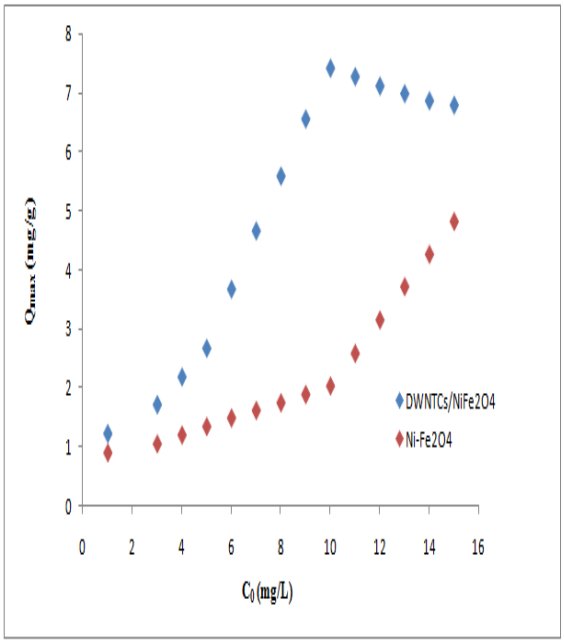

Figure 9. *Adsorption capacity of orange methyl on ($NiFe_2O_4$) and DWNTCs / $NiFe_2O_4$ as a function of the initial concentration*

V. Modeling Adsorption Kinetics

V.1. Kinetic model of the pseudo first order

The kinetic model of the pseudo first order [17] is represented by the following equation:

$$\ln(Q_e - Q_t) = \ln Q_e - k_1 \, t/2.303 \quad \ldots\ldots 2$$

Qe: amount adsorbed at equilibrium (mg.g^{-1}),
Qt: quantity adsorbed at time t (mg.g^{-1}),
K_1: pseudo first order rate constant (min^{-1}).

V.2. Model of the pseudo second order kinetics

The pseudo second model according to previous work of Ho and McKay [18] is described by equation (3) as follows:

$$\frac{t}{Q_t} = \frac{1}{Q_e} t + \frac{1}{k_2 Q_e^{\,2}} \quad \text{……..3}$$

Where:

Qe: amount adsorbed at equilibrium (mg. g^{-1}). Qt: quantity adsorbed at time (mg. g^{-1}). K_2: pseudo second order rate constant ($g.mg^{-1}.min^{-1}$).

Table 1 summarizes the parameters of the pseudo first order and second order models.

Table 1. *Parameters of pseudo first order and second order models*

Pseudo 1er ordre	**Pseudo 2eme ordre**
K_1=0.257	K_2 =0.287
Qe = 0.137 mg.g.$^{-1}$	Qe= 6.02 mg.g.$^{-1}$
Qe exp= 7.78 mg.g.$^{-1}$	Qe exp= 7.78 mg.g.$^{-1}$
R^2= 0.94	R^2= 0.99

The pseudo-first order model is widespread, and the kinetics indicate that the rate of solute removal as a function of time is directly proportional to the difference in saturation concentration, and the amount of adsorbed solute as a function of time [18, 19].

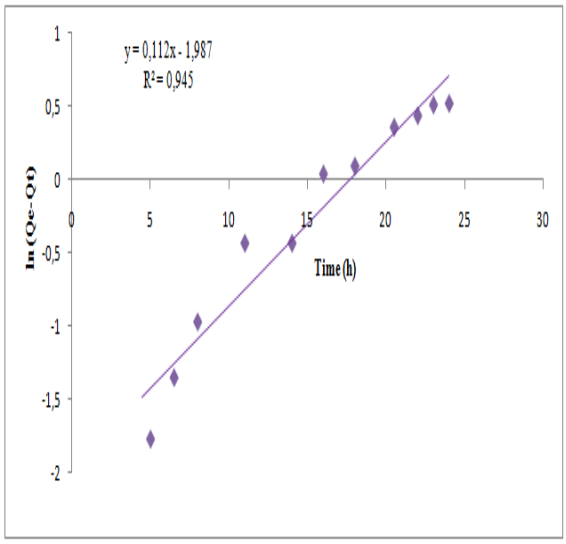

Figure 10. *Modeling the adsorption kinetics of orange methyl on the DWNTCs / $NiFe_2O_4$ by the pseudo first order model at pH = 5.*

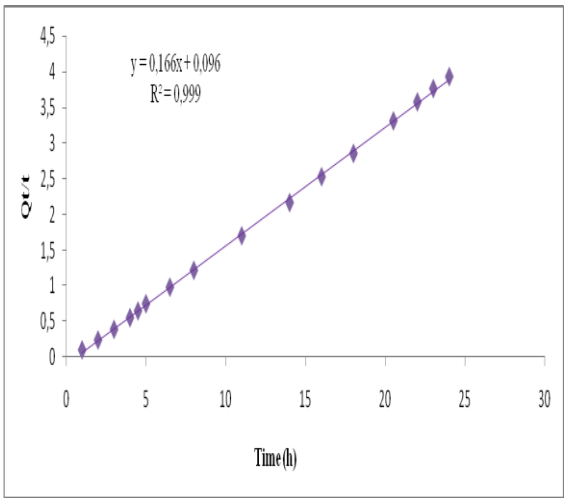

Figure 11. *Modeling the adsorption kinetics of orange methyl on the DWNTCs / $NiFe_2O_4$ by the pseudo second order model at pH = 5.*

The variation $\ln(Q_e - Q_t)$ as a function of time is not revealed linear and the regression coefficient R^2 is not satisfactory. Thereby, we noted that the adsorption kinetics do not respond to the Lagergren model of the pseudo first order, which allowed us to calculate the theoretical value of the adsorption capacity $Qe_{\,theo}$. Hence, the calculated value is very close to the experimental value, and we observed that adsorption of methyl orange on DWNTCs / $NiFe_2O_4$ discribe a second-order adsorption rate and chemical process [20]. Yet, by examining these values, generally the kinetics of adsorption describes pseudo second order model, with correlation coefficient of 0.99.

V.3. Modelling of adsorption isotherms

To describe the adsorption of the orange methyl studied, three models most frequently used are studied: Freundlich, Langmuir and Temkin. All the results were carried out at ambient temperature (25°C), pH 5 and an equilibrium time of 5 hours.

V.3.1. Freundlich Model

The Freundlich equation [20] is expressed by the following relation:

$$\log Q_e = \log K_F + n \log C_e \quad \text{…4}$$

By plotting log (Qe) = f (log Ce), the results obtained are represented in Figure 12 from which the slope of the line is n and the ordinate at the origin is log K_F.

Table 2. *Parameters of the modeling relating to adsorption isotherms of methyl orange on DWNTCs / $NiFe_2O_4$ at 25°C and pH 5.*

Freundlich model			Langmuir model			Temkin model		
1/n	K_F	R^2	Qm	b	R^2	A	B	R^2
0.77	279.25	0.97	5.78	1.25	0.76	$9.61*10^{14}$	$2.9*10^{-5}$	0.95

V.3.2. Model of Langmuir

Langmuir [21] proposes the following model

$$\frac{C_e}{Q_e} = \frac{1}{Q_m}.C_e + \frac{1}{Q_m.b} \quad \ldots\ldots\ldots\ldots 5$$

By plotting (Ce / Qe) = f (Ce), the results obtained are shown in Figure 13, where the slope of the line is 1 / Q_m and the ordinate at the origin is log 1 / Q_m.b.

V.33.Model of Temkin

The Temkin model [22] is represented by the following equation

$$Q_e = B.\ln K + B.\ln C_e \quad \ldots\ldots\ldots 6$$

Figure 14 represents the variation of Qe as a function of ln (Ce),
The correlation coefficients and adsorption parameters extracted from the linear plots of the three Freundlich, Langmuir and Temkin models after adsorption of methyl orange on DWNTCs / $NiFe_2O_4$ are summarized in the following Table 2.
As expected, the adsorption isotherm describes the relationship between the adsorbent and the adsorbate, *ie* the ratio between the adsorbed amount and the remaining one in solution [20].Accordingly, three models were studied namely Freundlich, Langmuir and Temkim where the parameters of the modeling are sumurized in Table 2. Analyzing the correlation coefficients, it has been found that the Freundlich isotherm has a correlation coefficient (R^2) of 0.97, Langmuir is of 0.76 and the Temkin model is of 0.95.

In the light of these results, the Freundlich model seems to describe adequately the adsorption of orange methyl on (DWNTCs/$NiFe_2O_4$). This result is in perfect agreement with the work of Ding [23] and his collaborators. According to Freundlich's isotherm theory, the ratio of solute adsorbed to a given mass of adsorbent for a concentration of solute in solution is not constant. This model is based on the relationship between the amount adsorbed and the concentration of the solute at equilibrium, and describing therefore a reversible adsorption and which is not limited to a monolayer, where it can be applied to describe adsorption on multilayers, with an adsorption and affinity distribution on a heterogeneous surface [24].

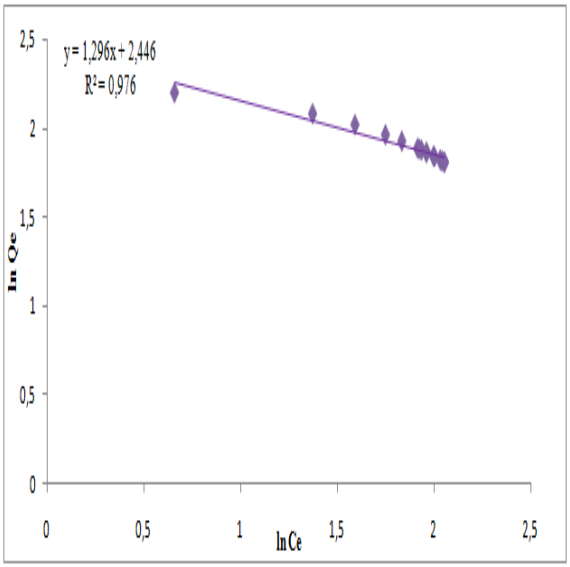

Figure 12. *Modeling the adsorption of methyl orange by the Freundlich model.*

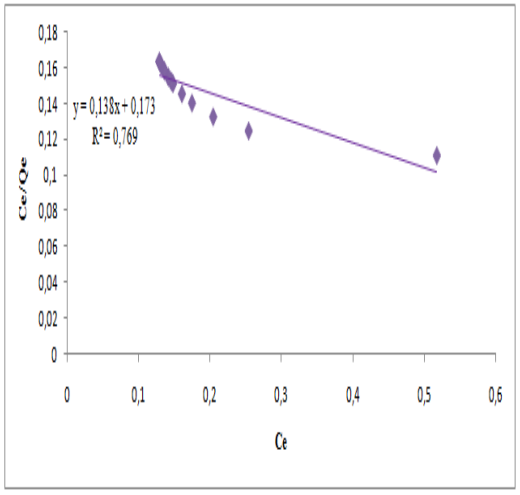

Figure13. *Modeling the adsorption of methyl orange by Langmuir model*

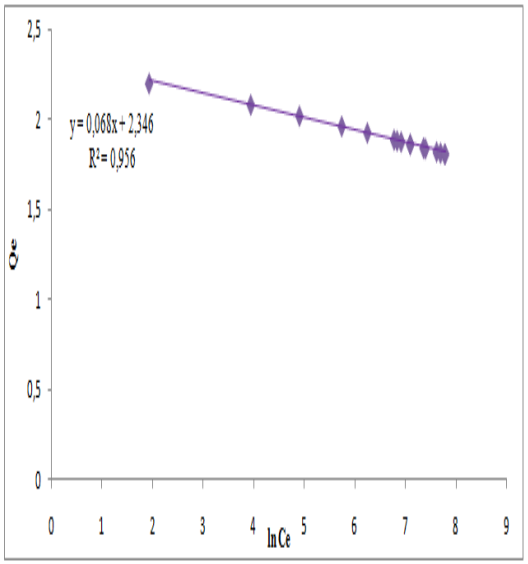

Figure 14. *Modelization of the adsorption of methyl orange by Temkin model*

VI. Conclusion

(DWNTCs / $NiFe_2O_4$) was used to remove methyl orange from contaminated water. The adsorbent was synthesized by hydrolysis using refluxing for 45min, where the nanocomposite characterization was achieved by Fourrier Transform Infrared Spectroscopy (FTIR), X-ray diffraction, surface-specific measurement, zeta potential and transmission electron microscopy (TEM). These techniques have indicated the existence of carbon nanotubes particles on one hand, and on the other hand the appearance of FeO molecules, which indicates the presence of $NiFe_2O_4$. The study of adsorption tests allowed us to demonstrate the effectiveness of (DWNTCs / $NiFe_2O_4$) in the removal of methyl orange, and we have evaluated the effectiveness adsorption capacity of 7.77 mg. l^{-1} for an equilibrium time of 5 h, pH 5, mass equal to 100 mg, an initial concentration of 10 mg. l^{-1} and a temperature of 25 °C. Overall, (DWNTCs / $NiFe_2O_4$) adsorbs twice better than $NiFe_2O_4$, which indicates the usefulness of carbon nanotubes in the nanocomposite. In addition, the adsorption kinetics of the dye on the (DWNTCs / $NiFe_2O_4$) describes the second-order kinetic model. The study of adsorption isotherms shows that the Freundlich isotherm describes with good agrement the adsorption of orange methyl on (DWNTCs / $NiFe_2O_4$). These encouraging results will provide insight to introduce an opportunity to achieve the removal of contaminants from water by nanocomposites materials.

VII. Référence

1. Jain, R.; Sikarwar, S. Photocatalytic and adsorption studies on the removal of dye Congo red from wastewater. International Journal of Environment and Pollution 27(2006)158–178.
2. Sanghi, R.; Bhattacharya, B. Review on decolorisation of aqueous dye solutions by low cost adsorbents. Coloration Technology. 118 (5) (2002) 256–269.
3. Abraham, T. Economics of ceramic magnets. The American Ceramic Society 73 (1994) 62–65.
4. Iijima S., Helical microtubules of graphitic carbon. Nature. 354(1991)56-58.
5. Dai,L.M.; Mau, A.W.H. Controlled synthesis and modification of carbon nanotubes and C60: carbon nanostructures for advanced polymeric composite materials. Advanced Materials 13(2001)899-913.
6. Flahaut, E.; Bacsa, R.; Peigney, A. Gram-scale CCVD synthesis of double walled carbon nanotubes. Chemical Commun 12 (2003) 1442-3.
7. Bortolamiol, T.; Lukanov, P.; Galibert, A-M.; Soula, B.; Lonchambon, P.; Flahaut, E. Double-Walled Carbon Nanotubes: Quantitative purification assessment, balance between purification and degradation and solution filling as an evidence of opening. Carbon 78(2014)79-90.
8. Maaz, K.; Karim, S.; Mumtaz, A.; Hasanain,S.K.; Liu,J.; Duan, J.L. Synthesis and magnetic characterization of nickel ferrite nanoparticles prepared by co-precipitation route. Journal of Magnetism and Magnetic Materials.321 (2009), 1838–1842.
9. Nejati, K., Zabihi, R. Preparation and magnetic properties of nano size nickel ferrite particles using hydrothermal method. Chemistry Central Journal 6 (2012)23.
10. Senthilkumar, B., Kalai Selvan, R., Vinothbabu, P., Perelshtein, I., Gedanken, A. Structural, magnetic, electrical and electrochemical properties of $NiFe_2O_4$ synthesized by the molten salt technique. Materials Chemistry and Physics 130 (2011)285–292.
11. Lingamdinne, L.P.; Koduru J.R .Studies on removal of Pb(II) and Cr(III) using graphene oxide based inverse spinel nickel ferrite nano-composite as sorbent. Hydrometallurgy .165 (2015)64-72.
12. Verma, K.C.; Singh, V.P.; Ram M., Shah J., Kotnala R.K. Structural, microstructural and magnetic properties of $NiFe_2O_4$, $CoFe_2O_4$ and $MnFe_2O_4$ nanoferrite thin films, J. Magn. Magn. Mater. 323 (2011) 3271- 3275.

13. T. Peng, X. Zhang, H. Lv, L. Zan, Preparation of $NiFe_2O_4$ nanoparticles and its visible – light-driven photoactivity for hydrogen production, Catal.Commun. 28 (2012) 116 – 119.
14. A. Jitianu, T. Cacciaguerra, R. Benoit, S. Delpeux, F. Beguin,S. Bonnamy, Synthesis and characterization of carbon nanotubes –TiO_2 nanocomposites, Carbon 42 (2004) 1147 – 1151.
15. Ahmed, D.S.; Haider, A.J.; Mohammad, M.R. Comparesion of functionalization of multi walled carbon nanotubes treated by oil olive and nitric acid and their characterization. Energy Procedia 36(2013)1111-1118.
16. Yu, CH.; Al-Saadi, A.; Shih, S.J.; Qiu, L. Immobilization of BSA on silica-coated magnetic iron oxide nanoparticle. Journal of Physical Chemistry C 113(2009) 537-543.
17. Ho,Y.S.; Mckay, G**.** Pseudo-second order model for sorption processes**.** Process Biochem. 34(1999)451-465.
18. [18] Bensacia, N., Fechete I., Moulay, S., Hulea, O., Boos, A., Garin, F. Kinetic and equilibrium studies of lead (II) adsorption from aqueous media by KIT-6 mesoporous silica functionalized with –COOH. Comptes Rendus Chimie. 17 (2014)869-880.
19. Bensacia, N.; Fechete, I.; Moulay, S.; Debbih-Boustila,S.; Boos, A.; Garin, F. Removal of cadmium (II) from aqueous media using COOH/TUD-1 mesoporous solid. Kinetic and thermodynamic studies. Environmental Engineering and Management Journal. 13(2014), 10, 2675-2686 .
20. Freundlich, H.M.F. Over the adsorption in solution. Journal of Physical Chemistry.57(1906) 385-470.
21. Langmuir, I. The constitution and fundamental properties of solids and liquids. Part I. Solids, Journal of American Chemical Society. 38 (1916) 2221-2295.
22. Temkin, M.I., Pyzhev, V. Kinetics of ammonia synthesis on promoted iron catalyst. Acta Physico-Chimica. 12(1940), 327–356.
23. Ding ,H.;Li ,X.; Wang, J.; Zhang, X . Adsorption of chlorophenols from aqueous solutions by pristine and surfacefunctionalized single-walled carbon nanotubes Journal of Environmental Sciences .43 (2016)187-98.
24. Moulay, S.; Bensacia, N. Removal of heavy metals by homolytically functionalized poly(acrylic acid) with hydroquinone. International Journal of Industrial Chemistry . 4(2016) 369–389.

Please cite this Article as:
Seffah K., Bensacia N., Skender AF., Flahaut E., Hadj-ziane-zafour A., *Synthesis and characterization of nano-magnetic material based on (carbon nanotubes / nickel ferrite): Application for the removal of methyl orange dye from contaminated water*, ***Algerian J. Env. Sc. Technology***, **3:1 (2017) 333-341**